doi:10.1111/evo.13886

Population history and the selective landscape shape patterns of osmoregulatory trait divergence in tidal marsh Savannah sparrows (*Passerculus sandwichensis*)

Phred M. Benham[1,2,3] and Zachary A. Cheviron[1]

[1]*Division of Biological Sciences, University of Montana, Missoula, Montana 59812*

[2]*Current Address: Museum of Vertebrate Zoology, University of California, Berkeley, 3101 Valley Life Sciences Building, Berkeley, CA 94720-3160*

[3]*E-mail: phbenham@berkeley.edu*

Received April 29, 2019
Accepted November 2, 2019

A persistent challenge in making associations between phenotypic and environmental variation is understanding how ecological factors and demographic history interact to shape adaptive outcomes. Evaluating the degree to which conspecific populations exposed to similar environmental pressures respond in parallel provides a powerful framework for addressing this challenge. We took this comparative approach with multiple populations of Savannah sparrows (*Passerculus sandwichensis*) found in tidal marshes along the Pacific coast of North America. The high salinities characterizing tidal marshes select for increased osmoregulatory performance and salinity tolerance. We collected data on physiological traits associated with osmoregulatory performance from 10 tidal marsh and three freshwater-adapted interior populations to evaluate the degree of parallel divergence across populations. All traits showed differences in the magnitude of divergence, but only total evaporative water loss (TEWL) showed differences in the direction of divergence. The drivers of these differences in both the magnitude and direction of divergence varied among traits. For kidney morphology and TEWL, patterns of divergence were best explained by variation in immigration rate from interior populations. Maximum temperature was the best predictor of variation in urine excretion ability, and both gene flow and temperature contributed to variation in plasma osmolality. Finally, analysis of multitrait divergence patterns indicated that differences in the direction of divergence were best explained by population genetic structure, whereas differences in the magnitude of divergence were explained by environmental differences. Together these results show that the influences of demography and the selective landscape can manifest themselves differently across functionally integrated traits.

KEY WORDS: **Adaptation, demography, geographic variation, nonparallelism, osmoregulation, tidal marshes.**

Strong correlations between environmental and phenotypic variation are ubiquitous in nature and suggest a strong role for local adaptation in driving spatial patterns of phenotypic diversity (e.g., Bergmann 1847; Allen 1877; Mayr 1963; James 1970; Graves 1991). Local adaptation occurs in response to spatially varying selective pressures that drive functional divergence in traits contributing to fitness, and it is most often recognized in cases where local individuals exhibit increased fitness compared to those from foreign populations (e.g., Kawecki and Ebert 2004; Savolainen et al. 2013). Although spatial variation in selective pressures operating on fitness differences among individuals ultimately drives local adaptation, interactions with nonselective forces such as demographic history and genomic architecture can influence patterns of adaptive divergence in complex ways (e.g., Kawecki and Ebert 2004; Savolainen et al. 2013). Understanding these complexities remains a major empirical challenge.

Conspecific populations that are exposed to similar ecological pressures can provide a natural experiment for teasing apart

the influences of different evolutionary processes on adaptation dynamics. Within this comparative framework, phenotypic responses to similar ecological pressures can vary along a continuum from completely parallel (multiple populations exhibit similarity in both the direction and magnitude of phenotypic divergence) to completely nonparallel divergence, where patterns of phenotypic divergence vary in both magnitude and direction (e.g., Stuart et al. 2017; Bolnick et al. 2018). Evaluating the degree of parallelism among populations along this continuum can thus provide valuable insights into the interactions among different microevolutionary processes, and how these interactions shape spatial patterns of phenotypic variation.

Although natural selection is the dominant force driving complete parallel evolution; a number of other processes, acting alone or in concert, can contribute to deviations from complete parallelism in the magnitude or direction of trait divergence. First, populations with smaller effective population sizes could exhibit reduced trait divergence because selection will operate less efficiently, and there will be lower levels of standing genetic variation available for selection to act upon (Wright 1982; Weber and Diggins 1990; Leimu and Fischer 2008; Agashe et al. 2011; Leinonen et al. 2012). Second, high rates of gene flow among populations that are locally adapted to different selective regimes will often constrain their adaptive phenotypic divergence (Slatkin 1987; Lenormand 2002; Nosil and Crespi 2004; Garant et al. 2007; Räsänen and Hendry 2008). Third, a longer history of exposure to selective pressures may lead to the evolution of novel solutions that move populations closer to adaptive peaks. In this case, populations exposed to selective pressures for longer will exhibit greater divergence in adaptive traits (Mopper et al. 2000; Beall 2006, 2007; Storz et al. 2010; Velotta et al. 2017). Finally, in natural populations, variation in the nature or magnitude of relevant selection pressures across qualitatively similar environments could also influence patterns of parallel divergence (e.g., Kaeuffer et al. 2012; Stuart et al. 2017). Thus, a full accounting of patterns of adaptive divergence requires the simultaneous quantification of ecological variation among populations and the characterization of key demographic parameters.

In addition to variation in demography and the selective landscape, genetic architecture (Yeaman and Whitlock 2011; Savolainen et al. 2013; Pfeifer et al. 2018), functional interactions among traits (e.g., many different traits contributing to a single function; Arnold 1983; Alfaro et al. 2005; Thompson et al. 2017), and/or phenotypic plasticity (Wund et al. 2008; Dalziel et al. 2015; Oke et al. 2016) of particular traits could all contribute to variation in the degree of parallelism both among traits and across populations. Indeed, multitrait analyses have shown a large degree of variation in patterns of parallelism among different traits within the same organism (e.g., Oke et al. 2017; Stuart et al. 2017; Langerhans 2018). However, in many of these studies, the measured traits contribute to multiple organismal functions (but see Thompson et al. 2017). Case studies that parse the influence of both ecological and demographic variation on divergence in interacting sets of traits contributing to a single aspect of organismal performance are needed to improve our understanding of the dynamic influences of demographic processes on adaptive evolutionary outcomes. Within this framework, a focus on the component traits underlying performance in a single aspect of organismal function should provide a more nuanced perspective on how potential drivers of nonparallelism interact within integrated systems to shape adaptive divergence. These insights, in turn, will provide a deeper understanding of the conditions that shape repeatable evolutionary outcomes.

In this study, we investigated the relative roles of demographic and ecological variation in shaping patterns of phenotypic divergence in a suite of traits that contribute to osmoregulatory performance in replicate populations of tidal marsh Savannah sparrows (*Passerculus sandwichensis*). Savannah sparrows are one of the most widespread songbird species in North America, breeding across a diverse array of environments from Arctic Canada to the Guatemalan highlands, including multiple populations that are resident in tidal marsh habitats along the Pacific coast of North America (Wheelwright and Rising 2008). Although many dietary details remain poorly studied, the daily inundations of saltwater into tidal marsh habitats is thought to increase the salt loads experienced by tidal marsh Savannah sparrows, both through the increased ingestion of osmoconforming, marine invertebrates (e.g., crustaceans and molluscans; DeRivera 2000; Wheelwright and Rising 2008), and at least occasional drinking of salt water (Benham, pers. obs.). Moreover, the osmotic stress experienced by sparrows is compounded by limited access to freshwater within the marshes, which will also select for osmoregulatory mechanisms to increase water conservation (Goldstein 2006). Given these osmoregulatory challenges, tidal marsh Savannah sparrows have long been an important study species for understanding the mechanisms that enable birds without salt glands, including all songbirds (order: Passeriformes), to cope with osmoregulatory stress (e.g., Cade and Bartholomew 1959; Poulson 1965; Johnson and Mugaas 1970; Goldstein et al. 1990; Casotti and Braun 2000; Walsh et al. 2019).

Early studies of Savannah sparrows demonstrated that individuals from tidal marsh habitats could maintain normal body weight with no mortality when drinking water that exceeded the normal salinity of seawater (0.6 M NaCl; Cade and Bartholomew 1959; Poulson and Bartholomew 1962), whereas interior conspecifics experienced substantial mortality (up to 60% of experimental individuals) when drinking water half the salinity of seawater (0.3 M NaCl). Subsequent work identified divergence in a number of physiological traits that contribute to this increase in salinity tolerance (Fig. 1). These include greater blood plasma

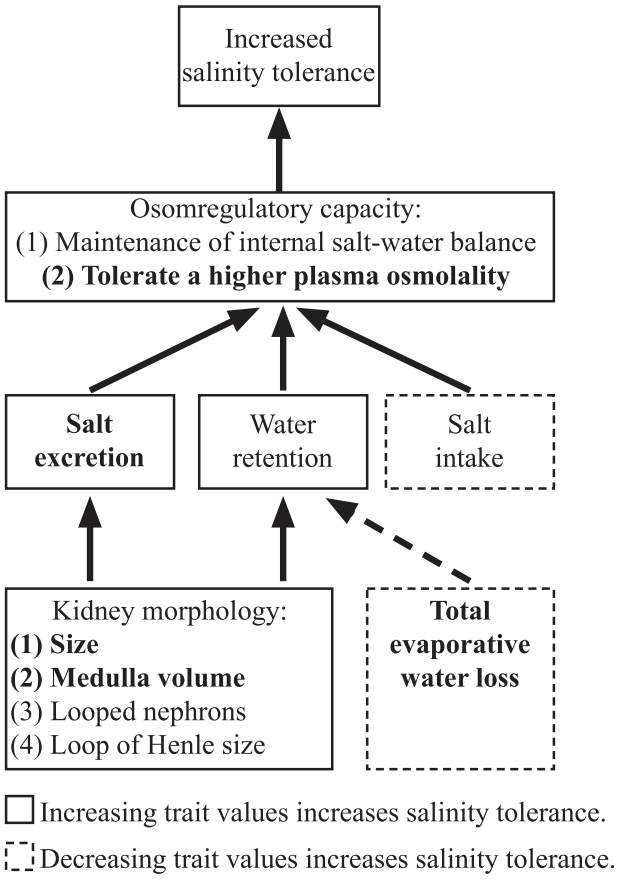

Figure 1. **Schematic showing how different traits contribute to the experimentally documented increases in salinity tolerance within Belding's Savannah sparrows. Solid boxes represent sets of traits that have been shown to increase in Belding's Savannah sparrow and this increase is thought to contribute to overall increases in salinity tolerance. Dashed boxes represent traits that have been shown or are thought to positively influence salinity tolerance when decreased in tidal marsh populations. Dashed arrow from total evaporative water loss indicates that this trait has not been measured in tidal marsh birds, but decreases in TEWL would be predicted to increase water retention. Traits written in bold denote traits that were measured in this study.**

osmolality levels, suggesting tolerance to higher internal osmolality, and a greater osmoregulatory capacity, which is the ability to maintain internally stable osmolality in the face of increased salt loads (Poulson and Bartholomew 1962; Goldstein et al. 1990). Tidal marsh birds also increase osmoregulatory capacity both through behavioral responses to reduce salt intake (Cade and Bartholomew 1959), and through an increased capacity to excrete salts in their urine (Poulson and Bartholomew 1962; Goldstein et al. 1990). Underpinning divergence in salt excretion capacity are a number of alterations in the morphology of tidal marsh sparrow kidneys, including overall increases in kidney size (Goldstein et al. 1990), increased medullary tissue (Poulson 1965; Johnson and Mugaas 1970; Johnson and Ohmart 1973), and greater area of the proximal and distal tubules of the loop of Henle (Casotti and Braun 2000). These modifications play a critical role in building up a steep osmotic gradient within the renal medulla via the countercurrent multiplier mechanism of the loop of Henle that enables increased salt excretion and water retention (Poulson 1965). Reducing water lost to evaporative cooling could also be an important mechanism of water conservation in tidal marsh birds. Several avian species that are native to desert environments exhibit reduced rates of evaporative water loss under heat stress (e.g., Dawson 1982; McKechnie and Wolf 2004; Williams and Tieleman 2005; Williams et al. 2012), yet patterns of evaporative water loss have not been measured in any tidal marsh bird species. Finally, acclimation responses to salinity treatments in Savannah sparrows and other songbirds show variation in the degree of osmoregulatory trait plasticity. This variation includes traits that (1) show no response to salinity treatments (e.g., plasma osmolality), suggesting a primarily genetic basis to trait variation; (2) traits that show evidence for both genetic and environmental influences on trait variation (e.g., medulla volume); and (3) traits, such as urine osmolality, that were highly plastic (summarized in Table S1).

This body of research provides a detailed understanding of the traits underlying enhanced osmoregulatory capacity in tidal marsh sparrows (Fig. 1), and provides expectations for how selection and demography might interact to shape patterns of divergence in these osmoregulatory traits. Eight Savannah sparrow subspecies occupy tidal marsh habitats from northern California south to Baja California and Sonora, Mexico (Fig. 2), yet the bulk of the physiological research performed thus far focuses on just a single subspecies, *P. s. beldingi* (but see Johnson and Ohmart 1973). Substantial variation in ecological variables and demographic histories likely exists across different tidal marsh populations of the Savannah sparrow, which may drive variation in adaptive divergence among the different tidal marsh subspecies. First, across the distribution of tidal marsh Savannah sparrows, precipitation, temperature, and salinity varies extensively with southern populations experiencing hotter and drier conditions, and generally higher salinities, all of which might exacerbate osmoregulatory stress and could result in greater divergence in traits associated with osmoregulatory performance. Second, demographic history also varies among tidal marsh populations with previous phylogeographic work indicating that tidal marshes were colonized at least twice by freshwater-adapted interior birds: (1) an older colonization of marshes in southern California and northwest Mexico and (2) a more recent colonization of the central California coast (Zink et al. 2005; Benham and Cheviron 2019). As a result, tidal marsh Savannah Sparrows provide an excellent opportunity to assess the ecological and demographic contributions to variation in osmoregulatory traits, and how complex interactions among these forces shape patterns of adaptive

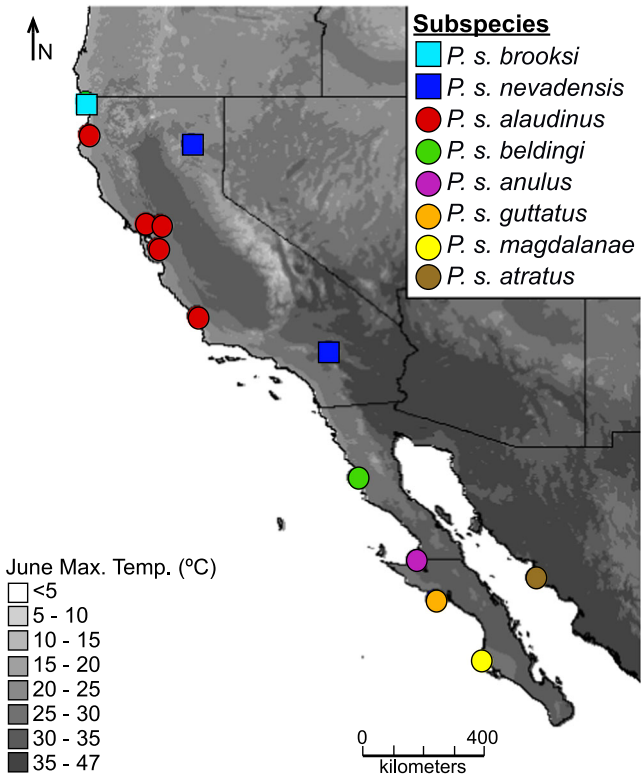

Figure 2. Map of California and northwest Mexico showing sampling localities for the study. Each point colored by subspecies distinction. Squares denote interior populations and circles tidal marsh populations. Grayscale of map reflects the maximum June temperature (°C) from the WorldClim dataset.

divergence. In this study, we measured a suite of traits associated with osmoregulatory performance (Fig. 1) in Savannah sparrows sampled from 10 tidal marsh and three freshwater-adapted interior populations. This physiological dataset is coupled with population genetic and environmental data to address the following questions: (1) to what degree have these traits diverged in parallel across the different tidal marsh populations? (2) How does variation in demographic parameters and the selective landscape contribute to variation in the degree of parallelism among traits and across populations?

Methods

Field sampling: We visited four separate tidal marsh localities in Mexico from May to June 2014 and we sampled five tidal marsh and three interior localities in California in May–June 2015 (Fig. 2). Each of the four Mexican localities was occupied by a distinct subspecies of Savannah sparrow: *P. s. anulus, P. s. guttatus, P. s. magdalanae,* and *P. s. atratus* (van Rossem 1947). We also included previously published data on kidney mass and plasma and urine osmolality for the subspecies *P. s. beldingi* (Goldstein et al. 1990). Four of the California tidal marsh localities were occupied by the subspecies *P. s. alaudinus*, whereas the fifth—Morro Bay—represents an apparent contact zone between *P. s. alaudinus* and *P. s. beldingi* (Benham and Cheviron 2019). Interior localities correspond to *P. s. brooksi* (Del Norte Co.) or *P. s. nevadensis* (Lassen Co., San Bernardino Co.; Grinnell and Miller 1944).

Physiological data: From each locality, 4–11 birds were captured using mist nets (see Table S2 for specimen voucher details). Immediately after capture, a urine sample was taken using a closed end cannula, with a small window cut in the side, inserted briefly into the cloaca (Goldstein and Braun 1989), and a blood sample was taken from the brachial vein. Blood samples were centrifuged to separate plasma and hematocrit. Blood and urine samples were flash frozen in liquid nitrogen to preserve samples for osmolality measurements in the laboratory (see below). Birds were held overnight to measure rates of total evaporative water loss (TEWL) and resting metabolic rate (RMR) using flow-through respirometry. The respirometry experiments involved placing birds in dark, 1-L open-circuit metabolic chambers with wire mesh above a thin layer of mineral oil to capture urine and feces. Chambers were placed in a thermal cabinet to maintain birds at a constant 28°C, which is within the thermal neutral zone of the species (Yarbrough 1971). Incurrent air was dried, using drierite (W.A. Hammond Drierite Co., Xenia, OH) before being pumped through animal chambers and a control chamber at constant rates (~500 mL/min). Upon exiting animal chambers air first passed through an RH-300 water vapor analyzer (Sable Systems, Inc., North Las Vegas, NV), air was then dried using drierite prior to entering a Foxbox gas analyzer (Sable Systems, Inc., North Las Vegas, NV) where we first measured carbon dioxide, followed by scrubbing CO_2 with ascarite and scrubbing additional water produced from the reaction of ascarite and CO_2 with drierite before measuring O_2 levels to assess RMR. We do not include RMR measures in downstream analyses as it did not significantly vary among populations and is not thought to contribute to increased salinity tolerance. Water vapor and gas measurements from the RH-300 and Foxbox were recorded continuously and differences in gas traces between the animal and control chambers were used to assess rates of water loss for each bird. Birds were allowed to adjust to chambers for 1 hour and then data were collected for 2 hours, while iteratively sampling air from the bird chamber for 15 minutes followed by 5 minutes of sampling from the control chamber. Following the respirometry measurements, birds were euthanized to collect muscle tissue, extract, and weigh whole kidneys (0.002 g precision balance) with the left kidney preserved in paraformaldehyde-glutaraldehyde solution for histological analyses (Karnovsky's Fixative; Electron Microscopy Sciences, Hatfield, PA). Data on kidney morphology were not collected from two sites in California (Morro Bay and Grizzly Island) as permit restrictions did not allow the sacrifice

of birds from these sites. All methods described here were approved by the University of Illinois, Urbana-Champaign IACUC (protocol #: 13418).

We measured osmolality (mOsmol/kg) for each urine and blood plasma sample using a Wescor® osmometer. The amount of salt birds were able to excrete was calculated as the ratio of urine: plasma osmolality (U:P ratio) where greater values of the U:P ratio are associated with a greater capacity to excrete salt and maintain salt–water balance (Bartholomew and Cade 1963). This can also reflect an individual's current salt–water balance, which depends on recent dietary inputs. Water vapor traces recorded from respirometry experiments were analyzed using the program Expedata by Sable Systems, Inc. (North Las Vegas, NV) to estimate TEWL (mg H_2O/g bird/hour). In this analysis, we converted data from relative humidity to mg/mL H_2O, corrected for flow rate (~500 ml/min.), and measured TEWL as the average value of a 5-minute nadir from the lowest and most stable 15 minutes sampling period. Measurements of kidney length and width were taken before and after embedding tissue in paraffin to account for shrinkage. All kidneys were embedded in paraffin wax using routine procedures (e.g. Casotti 2001). Using a microtome, six to eight transverse sections, 5 µm thick and ~1.5 mm apart, were taken from each kidney sample. Sections were stained with hemotoxylin and eosin for routine light microscopy. Images of the sections were digitized and volume estimates of the medulla and cortex were made using the Cavalieri point-counting method (Gundersen et al. 1988) in imageJ (Schneider et al. 2012).

Environmental data: We obtained bioclimatic data at 30-arc second resolution from the WorldClim dataset (Hijmans et al. 2005) to assess environmental differences among all specimen localities. These data were derived from interpolated climate surfaces available for the entire globe at 30-arc second spatial resolution and were gathered from several independent sources between 1950 and 2000. We used coordinates for each sampling locality to extract data from gridfiles on monthly minimum temperature (T_{min}), maximum temperature (T_{max}), and precipitation (Prec) within the program DIVA-GIS (http://www.diva-gis.org/). These monthly estimates were used to calculate average T_{min}, T_{max}, and Prec for the months of May and June when birds were sampled (Table S2). Finally, from each sampling locality we took one to five water samples randomly from different potential water sources (e.g., standing water, open estuary) and quantified osmolality (mOsmol/kg) for these samples using a Wescor® osmometer to estimate salinity for each locality (Table S3).

Genetic data: To infer population structure, migration rate, and effective population size for all populations, we extracted genomic DNA from 90 individuals (Table S2) from muscle tissue or whole blood using a Qiagen DNeasy Blood & Tissue extraction kit following the manufacturer's protocols (Valencia, CA). These individuals include 63 sampled during our fieldwork plus an additional 27 specimens from museum collections. Samples were sequenced using a double-digest, genotyping-by-sequencing (GBS) like approach (Parchman et al. 2012) to generate a large SNP dataset. See Benham and Cheviron (2019) for library preparation and sequencing details. Reads were demultiplexed, barcodes removed, and reads assembled into 89 bp "stacks" using the STACKS *de novo* pipeline (Catchen et al. 2011, 2013). Briefly, this pipeline involves assembling reads from each individual into stacks (hereafter referred to as RADloci), then matching RADloci across all individuals to generate a catalog of shared RADloci, and, finally, RADloci from all individuals were matched against the catalog and genotyped at this panel of loci. See Benham and Cheviron (2019) for further details on RADloci assembly and selection of parameters. Following assembly of reads into RADloci, we used the "populations" module (Catchen et al. 2013) within STACKS to calculate the summary statistics nucleotide diversity (based on formulae presented in Hohenlohe et al. 2010) and Fst (based on Weir and Cockerham 1984) among all 13 localities.

To make more direct inferences of effective population size, migration rate, and divergence times between each tidal marsh and interior population, we analyzed site frequency spectra (SFS) within the program ∂a∂i (Gutenkunst et al. 2009). For each comparison, we consider all individuals from the three interior populations as a single freshwater-adapted interior population. Previous demographic analyses suggest these interior localities are all part of a large panmictic population that spans much of North America (Benham and Cheviron 2019). To minimize the influence of sequencing errors on the SFS for each population pair, we filtered VCF files to only include SNPs with read depth ≥ 6 and that were in Hardy–Weinberg equilibrium (α set to 0.05). This resulted in final datasets for each tidal marsh-interior comparison comprising 3190–5421 SNPs. Filtered VCF files were then converted to ∂a∂i input files using the vcf2dadi function in the R package stackr version 0.2.6 (Gosselin and Bernatchez 2016). Analyses were based on a folded SFS given lack of quality genomic data from a suitable outgroup.

For each tidal marsh population-interior comparison, we fit an isolation-with-migration (IM) model to the SFS. Our primary goal was to infer migration rates, effective population sizes, and divergence times and not necessarily infer the most likely demographic history for each population, thus we did not explore other demographic models (e.g., exponential growth and bottlenecks). Previous demographic analyses using the SNPs from the same individuals suggested that populations within nominate Savannah sparrows (population that encompasses all interior populations sampled and birds from coastal California) experienced a constant population size through time with no evidence for fluctuations in population size (Benham and Cheviron 2019). Finally, exploratory ∂a∂i analyses on these datasets suggested that models with migration were a better fit to the observed SFS,

then models without migration parameters. For each tidal marsh to interior population comparison, 10 optimizations were run from different starting parameters using the perturb function in ∂a∂i with max number of iterations set to 10. To ensure that a global optimum for a given model had been reached, we ran one final optimization with 50 iterations using the parameter values estimated from the shorter run with the highest likelihood. We calculated demographic parameter values from the estimated value of theta ($4N_e\mu L$; L is sequence length) based on a 1-year generation time for Savannah sparrows (Wheelwright and Rising 2008), the average substitution rate for Passeriformes: 3.3×10^{-9} substitutions/site/year (Zhang et al. 2014), and total sequence length equal to the number of loci times 89-bp (the length of each locus). We calculated uncertainty for parameter estimates using a nonparametric bootstrapping approach: sampling with replacement over all loci, generating frequency spectra from 100 resampled SNP datasets, and using these spectra to calculate parameter uncertainties using the Godambe information matrix (GIM) in ∂a∂i (Coffman et al. 2016).

DATA ANALYSIS

Previous phylogeographic studies of the Savannah sparrow indicated that tidal marsh populations derived from two independent colonization events: (1) birds from southern California and Mexico (hereafter termed Mexico tidal marsh) and (2) those sampled from the central California coast (hereafter termed California tidal marsh) (Benham and Cheviron 2019). The Mexico tidal marsh populations diverged from their interior ancestors approximately 480,000 ybp (95% CI: 240,829–2,066,377 ybp), whereas the central California populations were not genetically differentiated from interior populations. To determine the influence of these different population histories on adaptive divergence in each of the osmoregulatory traits measured, we first analyzed sampling localities as three groups: (1) Mexico tidal marsh, (2) California tidal marsh, and (3) interior California. We calculated effect size (Cohen's D) for each trait based on t-tests between California tidal marsh and the interior and between Mexico tidal marsh and interior. We further evaluated statistical differences among the three groups using one-way analysis of variance (ANOVA) and Tukey honest significant difference (HSD) post hoc tests. All statistical analyses were performed in the open source program R version 3.5.1 (https://www.r-project.org/).

Although sampled tidal marsh populations stem from only two colonization events (Mexico and Central California) (Benham and Cheviron 2019), gene flow rates, effective population sizes, and environmental variables could vary among populations within the two colonizing lineages and influence patterns of phenotypic divergence among populations within each lineage. To dissect the relative influence of environmental and demographic variation on trait divergence among all 10 sampled tidal marsh populations, we used a structural equation modeling (SEM) approach. Divergence for each osmoregulatory trait is measured as the difference between the trait mean for each tidal marsh population and the average across all individuals from the three interior populations (i.e., a single trait mean value from the interior). All ecological, demographic, and phenotypic variables were z-transformed prior to analyses. For each SEM model, we measured the influence of migration rate and a latent variable "ecological differences" on the response variable, osmoregulatory trait divergence (Fig. 3). Preliminary regression analyses found that variation in effective population size was not significantly correlated with variation in any of the six osmoregulatory traits among the 10 tidal marsh populations with the exception of a negative correlation between Ne and plasma osmolality (Fig. S1). In the case of plasma osmolality, the negative relationship is also opposite the predicted positive influence of Ne on trait divergence. Given these results and potential reductions in statistical power with the addition of more parameters, we excluded Ne from the model. The latent variable ecological differences were inferred from four observed ecological variables: minimum salinity, May–June T_{max}, May–June T_{min}, and May–June Prec. The estimated beta coefficients for migration rate and ecological differences were used to estimate the relative contributions of these two components on variation in trait divergence, while controlling for covariance between the migration rate and ecological differences (Fig. 3). Analysis of the model was performed using maximum-likelihood estimation in the "lavaan" R package (Rosseel 2012). We also corrected for spatial autocorrelation among the predictor variables using Moran's I implemented in the function "lavSpatialCorrect" (https://github.com/jebyrnes/spatial_correction_lavaan). For each trait, we also performed a series of regression analyses between migration rate and trait divergence where we compared the fit of both a linear and second-order polynomial model.

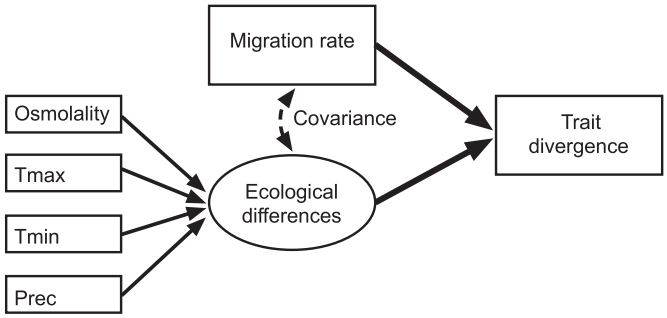

Figure 3. Model tested using structural equation modeling to dissect the relative influence of ecological variation and migration rate on variation in divergence in the six measured traits associated with osmoregulatory performance. Variation in osmolality, May–June maximum temperature (T_{max}), May–June minimum temperature (T_{min}), and May–June precipitation (Prec) contribute to the latent variable ecological differences.

We also assessed the relationship between May–June maximum temperature and trait divergence using linear regression analyses.

The measured traits likely interact in important ways to contribute to overall osmoregulatory performance (Fig. 1) and at least some of the traits show significant patterns of collinearity (Fig. S2). To account for these interactions among osmoregulatory traits, we also assessed the influence of gene flow and environmental variation on patterns of osmoregulatory divergence within a vector-based, multivariate framework (e.g., Adams and Collyer 2009; Stuart et al. 2017). Briefly, this method involves comparing vectors connecting multivariate phenotypic means (centroids) between two populations in different environments. For each vector, the vector length describes the magnitude of divergence between populations and vector direction reflects the relative importance of certain traits in contributing to divergence. The metrics vector direction and length can be used to characterize the degree to which populations exhibit parallel divergence in multivariate trait space with population pairs being completely parallel if vector lengths and direction are identical, whereas deviations from parallelism can be quantified as differences in either the direction or magnitude of vectors.

We inferred vectors of divergence between all interior individuals and each tidal marsh population for the six phenotypic traits, environmental variables, and genetic distance between populations. Following Stuart et al. (2017), we calculated *t*-tests for each trait between all interior individuals and each tidal marsh population. The angle of divergence (θ) between the vectors for each population was then calculated based on the arccosine of the correlation coefficients of trait *t*-statistics. The magnitude of divergence (L) for each population vector was calculated as a summary of the *t*-statistics calculated for each trait, and ΔL was calculated based on the pairwise differences in L among all tidal marsh populations. We took a similar approach to calculate vectors of environmental divergence. To calculate vectors of genetic divergence, we performed a principal components analysis on a dataset of 66,705 SNPs exported from vcftools in 012 format with missing data imputed using the mean allele frequency of the entire dataset for the missing SNP position. We performed a principal components analysis on this dataset and retained data from all principal components. Plotting the first two principal components produced results that are similar to published patterns of population genetic structure (Benham and Cheviron 2019). We calculated centroids for each population across all of the principal components axes from the PCA. Genotype vectors were then generated based on the distance between centroids of each tidal marsh population and the interior populations. These vectors from each marsh population were then used to calculate θ, L, and ΔL for genetic distance. Finally, we used partial Mantel tests (using the partial.mantel.test command from ncf r package) using 10,000 permutations to compare correlations between θ and ΔL for genetic distance, environmental divergence, and multivariate phenotypic divergence. All multivariate analyses were performed in R using scripts provided with Stuart et al. (2017).

Results

VARIATION IN PHYSIOLOGICAL TRAITS AMONG TIDAL MARSH POPULATIONS

Across the different populations, most trait values were greater in the two tidal marsh populations relative to interior birds, with the Mexico tidal marshes exhibiting a trend toward greater divergence from the interior population than those from the California tidal marshes (Table S4; Fig. 4). For most traits, the effect sizes calculated from comparisons between tidal marsh and interior populations were in the expected direction of divergence for both tidal marsh groups (California and Mexico). Mexico tidal marsh birds exhibited greater divergence from interior birds in kidney mass, medulla volume, plasma osmolality, urine osmolality, and only Mexico tidal marsh birds exhibited significant increases in the Urine:Plasma osmolality ratio (Fig. 4). TEWL was not significantly different between the interior and Mexican tidal marsh populations, but rates of TEWL were greater in California tidal marshes than interior birds, opposite of the prediction that TEWL should be reduced in freshwater-limited tidal marsh habitats. These patterns were corroborated by one-way ANOVA and post hoc analyses, which showed that both Mexico and California tidal marsh birds were significantly different from interior populations in mean kidney mass (cal: $P = 0.02$, Cohen's $D = 1.56$; mex: $P < 0.0001$, Cohen's $D = 2.69$) and plasma osmolality (cal: $P = 0.0001$, Cohen's $D = 1.46$; mex: $P < 0.0001$, Cohen's $D = 2.53$); however, only the Mexican tidal marsh populations were significantly divergent from interior birds in medulla volume (cal: $P = 0.8$, Cohen's $D = 0.73$; mex: $P < 0.0001$, Cohen's $D = 2.67$) and urine osmolality (cal: $P = 0.9$, Cohen's $D = 0.14$; mex: $P = 0.015$, Cohen's $D = 0.94$; Fig. 4). Moreover, based on Tukey HSD post hoc tests, Mexican populations had significantly larger kidney mass ($P < 0.0001$), medulla volume ($P < 0.0001$), and plasma osmolality than the California tidal marsh birds ($P < 0.0001$). Neither California nor Mexico statistically differed from the interior in the U:P ratio, although Mexican birds did exhibit greater divergence in this metric (cal: $P = 0.97$, Cohen's $D = -0.08$; mex: $P = 0.06$, Cohen's $D = 0.65$; Fig. 4).

PATTERNS OF GENETIC DIVERSITY

Across the 10 tidal marsh populations, nucleotide diversity (π) increased from south-to-north with populations from Sonora, Mexico, and southern Baja California exhibiting the lowest π (0.0012–0.0013) and populations from northern California exhibiting levels of π comparable to interior populations (0.0028–0.0029). Genetic divergence as measured by mean Fst between

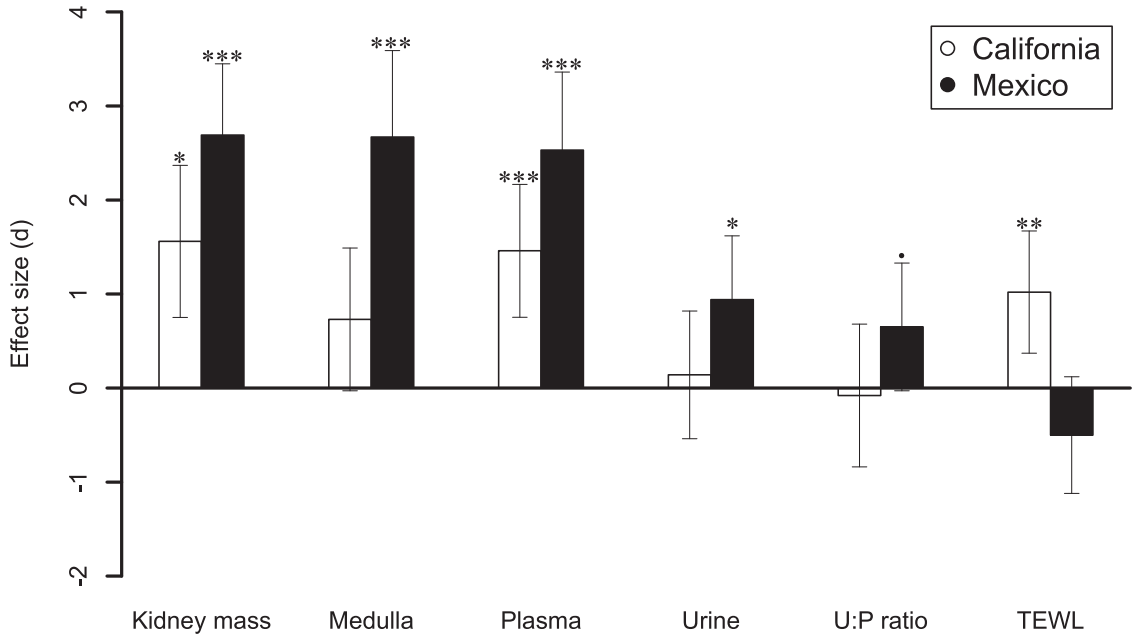

Figure 4. Plot of effect sizes for each trait. Zero line represents mean trait value from the three interior populations. Effect size was calculated using Cohen's *D* based on *t*-tests from between California tidal marsh and interior or Mexico tidal marsh and interior. Traits are kidney mass corrected for variation in body size, volume of medulla tissue in the kidneys (mm^3), plasma osmolality (mOsmol/kg), urine osmolality (mOsmol/kg), ratio between urine and plasma osmolality, and total evaporative water loss (TEWL) (mg/g/hour). Asterisks denote results from ANOVA and Tukey HSD post hoc analyses of the three groups (interior, Mexico tidal marsh, California tidal marsh). * < 0.001; ** <0.01; * <0.05; • = 0.06.**

the three interior and each coastal population showed the opposite trend; southern tidal marsh populations exhibited the greatest Fst (0.12), whereas the northern populations exhibited the lowest (0.041–0.059). Effective population sizes (Ne), estimated from fitting an isolation with migration model to the SFS in ∂a∂i, showed similar trends to π with populations from northern California exhibiting larger population sizes (mean: 141,782; range: 87,397–269,934) than populations from northwest Mexico (mean: 60,073; range: 37,434–94,099) (Table 1). Migration rate from interior populations into tidal marsh populations also declined from North-to-South along the Pacific coast similar to patterns of Fst (Table 1). Tidal marsh populations from northern California experienced an average per generation immigration rate (m) from interior populations of 4.69×10^{-5} m, whereas Mexican tidal marsh populations experienced lower average immigration rates of 1.29×10^{-6} m (Table 1). Fst was found to be significantly correlated with ∂a∂i estimates of migration rate ($R^2 = 0.714$, $P = 0.0013$), but not estimates of divergence time ($R^2 = 0.246$, $P = 0.083$) (Fig. S3).

THE ROLE OF DEMOGRAPHIC VERSUS ECOLOGICAL FACTORS SHAPING PHYSIOLOGICAL VARIATION

SEM analyses showed migration rate to be the only significant predictor of variance in kidney mass (-0.722 ± 0.298) and TEWL (0.679 ± 0.197) divergence (Table 2). In contrast, ecological differences explained a greater amount of variance in urine osmolality (0.724 ± 0.190) and urine:plasma osmolality ratio (0.51 ± 0.199). Both migration rate and ecological differences contributed significantly to variation in plasma osmolality (migration rate: -0.528 ± 0.160; ecological differences: 0.497 ± 0.161). Neither migration rate nor ecological differences significantly explained divergence in medulla volume; however, when Fst instead of migration rate was included as a predictor variable in the model, Fst did explain latitudinal variation in medulla volume divergence (Table S5). Performing a correction for spatial autocorrelation using Moran's I did not influence results for the most part, with two exceptions. One, the statistically significant relationship between ecological differences and plasma osmolality was no longer supported, and two, there was no longer a significant relationship between kidney mass and migration rate (Table 2). Regression analyses show similar patterns with migration rate significantly correlated with kidney mass, medulla volume, plasma osmolality, and TEWL, but not urine osmolality or the urine:plasma osmolality ratio (Fig. 5). Rather, maximum temperature was strongly correlated with urine concentrating ability traits (Fig. 6).

The multivariate, vector-based analyses showed that pairwise directions of phenotypic divergence (θ) varied from 3.32° to 126.45° (mean: 64.60°, SD: 35.86°) and the pairwise differences in the magnitude of divergence (ΔL) ranged from −12.16 to 8.45 standard error units (mean: −1.91, SD: 4.95). Variation in

Table 1. Population genetic parameters for the 10 tidal marsh populations of Savannah sparrow inferred from analysis of the site frequency spectrum in ∂a∂i.

Population	N_{ref}	N_e tidal	N_e upland	T_{sp}	Upland –> tidal	Tidal –> upland
Humboldt Bay	19,795 (±10,249)	138,328 (±103,781)	625,997 (±171,708)	218,640 (±68,523)	4.93×10^{-05} ($\pm 5.0 \times 10^{-05}$)	2.13×10^{-05} ($\pm 6.9 \times 10^{-06}$)
San Pablo Bay	23,612 (±9635)	122,019 (±41,830)	624,400 (±141,641)	228,661 (±55,583)	4.65×10^{-05} ($\pm 3.3 \times 10^{-06}$)	5.47×10^{-06} ($\pm 1.7 \times 10^{-05}$)
Suisun Bay	13,535 (±8362)	87,397 (±33,866)	664,641 (±200,294)	243,973 (±86,735)	7.12×10^{-05} ($\pm 2.9 \times 10^{-05}$)	8.94×10^{-07} ($\pm 1.7 \times 10^{-06}$)
San Francisco Bay	13,037 (±11,347)	228,642 (±53,746)	611,627 (±542,584)	264,706 (±180,504)	1.29×10^{-05} ($\pm 4.4 \times 10^{-06}$)	1.02×10^{-05} ($\pm 3.7 \times 10^{-06}$)
Morro Bay	27,533 (±9014)	91,230 (±15,769)	624,143 (±99,412)	207,091 (±41,491)	4.66×10^{-06} ($\pm 1.5 \times 10^{-06}$)	4.60×10^{-06} ($\pm 1.6 \times 10^{-06}$)
Bahía San Quintin	18,208 (±8747)	94,099 (±24,821)	685,741 (±164,598)	227,757 (±65,518)	3.91×10^{-06} ($\pm 1.7 \times 10^{-06}$)	3.26×10^{-06} ($\pm 9.9 \times 10^{-07}$)
Guerrero Negro	16,329 (±7118)	71,451 (±22,430)	743,120 (±152,322)	237,087 (±70,812)	2.49×10^{-06} ($\pm 1.7 \times 10^{-06}$)	2.99×10^{-06} ($\pm 9.3 \times 10^{-07}$)
Punta Abreojos	8903 (±8775)	57,708 (±37,876)	696,076 (±345,479)	278,646 (±159,155)	1.20×10^{-09} ($\pm 8.9 \times 10^{-07}$)	4.25×10^{-06} ($\pm 1.9 \times 10^{-06}$)
Lopez Mateos	51,002 (±156,652)	39,673 (±73,121)	803,620 (±1,228,172)	1,190,437 (±282,258)	1.10×10^{-09} ($\pm 1.2 \times 10^{-05}$)	7.84×10^{-06} ($\pm 1.0 \times 10^{-06}$)
La Atanasia	23,906 (±5134)	37,434 (±22,338)	796,585 (±149,296)	627,789 (±9189)	5.80×10^{-08} ($\pm 2.7 \times 10^{-06}$)	7.68×10^{-06} ($\pm 9.9 \times 10^{-07}$)

N_{ref} refers to ancestral population size. N_e tidal is the estimated effective population size for tidal marsh birds and N_e upland the effective population size estimated for the three upland populations combined. T_{sp} is divergence time between upland and each tidal marsh population. Finally, migration rates are shown in direction from upland to tidal marsh and tidal marsh to upland.

θ of phenotype was significantly explained by variation in both θ of environment ($R^2 = 0.473$; $P = 0.009$; Fig. 7A) and θ of genetic distance ($R^2 = 0.536$; $P = 0.002$; Fig. 7B). However, partial Mantel tests only found a significant relationship between θ phenotype and θ genetic distance when controlling for θ environment ($R^2 = 0.407$; $P = 0.019$), but not θ phenotype and θ environment when controlling for θ genetic distance ($R^2 = 0.304$; $P = 0.072$). Variation in vector length (L) between tidal marsh and interior habitats was significantly explained only by environmental L ($R^2 = 0.645$; $P = 0.006$; Fig. 7C) and not genetic L ($R^2 = 0.26$; $P = 0.09$; Fig. 7D). Finally, pairwise differences in the magnitude of phenotypic divergence among populations (ΔL) was significantly explained by both differences in environment ΔL ($R^2 = 0.803$; $P = 0.0004$; Fig. 7E) and genetic distance ΔL ($R^2 = 0.514$; $P = 0.0012$; Fig. 7F). However, unlike θ phenotype, partial Mantel tests only identified a significant relationship between phenotype ΔL and environment ΔL when controlling for genetic ΔL ($R^2 = 0.734$; $P = 0.0004$), but not phenotype ΔL and genetic ΔL when controlling for environment ΔL ($R^2 = -0.205$; $P = 0.133$). Together these results suggest that variation in the direction of genetic divergence among tidal marsh populations best explains multivariate variation in the direction of divergence for osmoregulatory traits, whereas variation in environment among sites best explains differences in the overall magnitude of divergence.

Discussion

The observed outcomes of local adaptation reflect complex interactions among many ecological and evolutionary processes that can influence the degree of divergence across functionally integrated traits. This inherent complexity in adaptive divergence makes the accurate interpretation of geographic variation challenging and necessitates approaches with the power to distinguish potential drivers of population divergence. To address this issue, we analyzed divergence patterns across 10 tidal marsh and three freshwater-adapted, interior populations of the Savannah sparrow. Across the 10 tidal marsh populations, divergence from interior populations occurred in the same direction for most traits with the exception of TEWL. However, the magnitude of trait divergence was greater in populations sampled from tidal marshes in northwest Mexico compared to those in California (Fig. 4). Trait-specific analyses showed that this variation in trait divergence among sites was best explained by variation in gene flow in some traits (e.g., medulla volume), but variation in the selective landscape in others (e.g., urine osmolality; Table 2). Variation in both genetic distance and the strength of relevant selective pressures also contributed to patterns of multivariate divergence with genetic distance influencing variation in the direction of phenotypic divergence, but variation in the magnitude of environmental differences best explaining variation in the magnitude of phenotypic

Table 2. Structural equation modeling results examining relative influence of environment and migration rate on trait divergence across the 10 sampled tidal marsh populations (see Fig. 2).

	No correction			Ecological variables				Spatial correction	
Trait	Migration ± SE	Ecology ± SE	Cov.	Salinity	T_{max}	T_{min}	Prec	Migration	Ecology
Kidney mass	$-0.722 \pm 0.298^{*}$	0.337 ± 0.221 ns	−0.57	0.524	1	0.869	−0.84	−0.49 ns	0.45 ns
Medulla volume	-0.636 ± 0.418 ns	0.292 ± 0.313 ns	−0.68	0.571	1	0.893	−0.85	−0.54 ns	0.33 ns
Plasma osmolality	$-0.528 \pm 0.16^{**}$	$0.497 \pm 0.161^{**}$	−0.33	0.325	1	0.859	−0.68	-0.53^{*}	0.50 ns
Urine osmolality	0.141 ± 0.181 ns	$0.724 \pm 0.19^{***}$	−0.24	0.193	1	0.801	−0.69	0.14 ns	0.72^{***}
Urine:plasma ratio	0.077 ± 0.214 ns	$0.51 \pm 0.199^{*}$	−0.09	−0.08	1	0.642	−0.58	0.09 ns	0.51^{*}
TEWL	$0.679 \pm 0.197^{**}$	-0.230 ± 0.18 ns	−0.49	0.50	1	0.903	−0.70	0.71^{***}	−0.26 ns

For each trait, the estimated coefficients for migration rate and the latent variable ecology plus or minus the standard errors (SE) are presented as well as the covariance between migration rate and ecology (cov). Salinity, May–June maximum temperature (T_{max}), May–June minimum temperature (T_{min}), and May–June precipitation (Prec) were the four variables used to generate the latent variable ecology, presented are factor loading coefficients for each variable. Also shown are coefficients and significance for migration rate and ecology following correction for spatial autocorrelation.
$^{***}P < 0.001$; $^{**}P < 0.01$; $^{*}P < 0.05$; ns > 0.05.

divergence. These results emphasize the value of quantifying the degree of parallel divergence among populations to understand how the selective landscape, demography, and functional relationships among traits interact to shape spatial patterns of phenotypic divergence.

PATTERNS OF GEOGRAPHIC VARIATION IN TRAITS ASSOCIATED WITH OSMOREGULATORY PERFORMANCE

Past physiological work in Savannah sparrows identified a suite of traits associated with differences in salinity tolerance between interior and tidal marsh Savannah sparrows, these include increases in kidney size (Johnson and Mugaas 1970; Goldstein et al. 1990; Casotti and Braun 2000); medullary volume (Johnson and Mugaas 1970; Casotti and Braun 2000); number of medullary cones (Poulson 1965); area of proximal and distal tubules of the loop of Henle, collecting duct, and kidney capillaries (Poulson 1965; Casotti and Braun 2000); and plasma osmolality and urine osmolality (Cade and Bartholomew 1959; Poulson and Bartholomew 1962; Goldstein et al. 1990). The bulk of this work has focused on a single tidal marsh subspecies, *P. s. beldingi* (but see Johnson and Ohmart 1973). We sampled an additional five subspecies of Savannah sparrow that occupy tidal marshes and found that divergence in osmoregulatory traits from interior birds, while often in the same direction (with the exception of TEWL), differed in magnitude, with an overall trend of reduced divergence in the central California coast populations relative to *P. s. beldingi* and other Mexican tidal marsh populations (Fig. 4). This finding highlights the value of revisiting ecological and evolutionary physiology studies with increased geographic sampling to develop a more nuanced understanding of physiological divergence among populations.

Although a reduced reliance on evaporative water loss for thermoregulation is a widely documented adaptation to desert environments (e.g., Dawson 1982; McKechnie and Wolf 2004; Williams and Tieleman 2005; Williams et al. 2012), whether similar adaptations exist in other freshwater-limited environments, such as tidal marshes, had been previously unstudied. We found that in Mexican tidal marsh populations TEWL was significantly reduced relative to interior birds (apart from interior birds sampled in the San Bernardino Mountains, CA; Table S4); however, tidal marsh populations from the central California coast generally exhibited greater TEWL than the three interior populations (Fig. 4). These results suggest that water conservation via reduced evaporative cooling may be important for adaptation to tidal marshes under some ecological and/or demographic conditions (see below), but is not a universal response to high salinity.

DEMOGRAPHIC VERSUS ECOLOGICAL DRIVERS OF OSMOREGULATORY TRAIT DIVERGENCE

Observed differences in the magnitude of trait divergence among tidal marshes (Fig. 4) could reflect variation in demographic history, the abiotic selective landscape (e.g., differences in temperature, precipitation), or both. Based on our trait-specific analyses, we found that the relative influence of these factors was trait dependent. For kidney mass, medulla volume, plasma osmolality, and TEWL, we found a significant, negative relationship between migration rate and the magnitude of trait divergence from interior populations (Table 2; Fig. 5). Gene flow from maladapted individuals immigrating into a population is predicted to constrain adaptive divergence (Slatkin 1987; Hendry et al. 2001; Lenormand 2002), and our results are consistent with several other empirical studies documenting this negative influence of gene flow on trait divergence (e.g., Nosil and Crespi 2004; Postma and

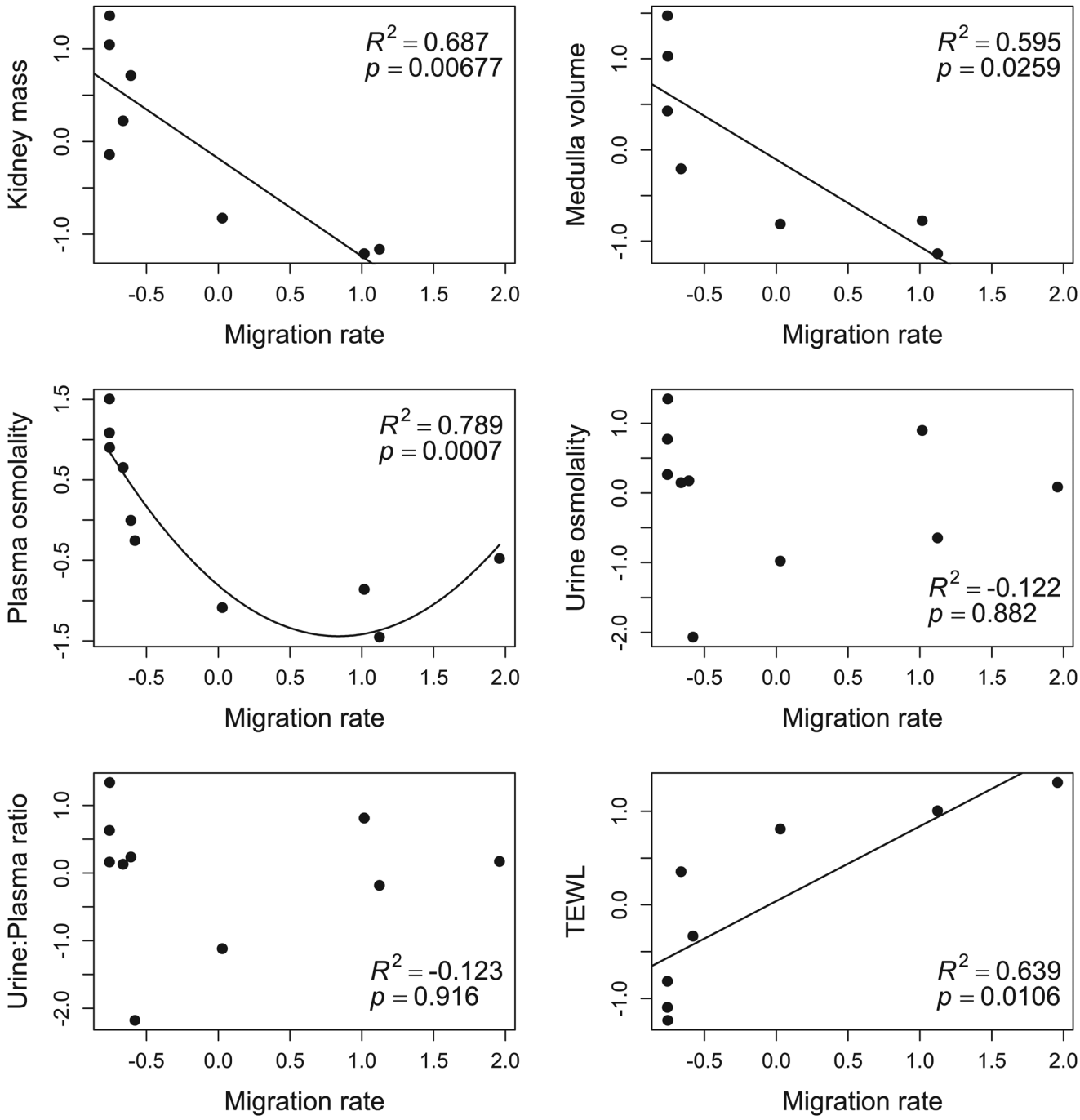

Figure 5. **Linear regression results showing the relationship between migration rate and each of the measured osmoregulatory traits. All values are *z*-transformed.**

Noordwijk 2005; Räsänen and Hendry 2008; Raeymaekers et al. 2014; Benham and Witt 2016; Stuart et al. 2017). Although gene flow into peripheral populations can also have a positive influence through the influx of genetic diversity into an inbred population at marginal range edges (e.g., Whiteley et al. 2015; Fitzpatrick et al. 2016), our results do not support a positive influence of gene flow on adaptive divergence in tidal marsh Savannah sparrows. Analyses of multivariate, osmoregulatory divergence found that the angle of multitrait divergence varied from highly parallel vectors of divergence (minimum angle of divergence ~3°) to nonparallel vectors (maximum angle, ~126°). This variation in the degree of phenotypic parallelism was best explained by patterns of genetic structure, which further supports an important role for population history (i.e., colonization time, migration rate) in shaping patterns of adaptive divergence within the osmoregulatory system of tidal marsh sparrows.

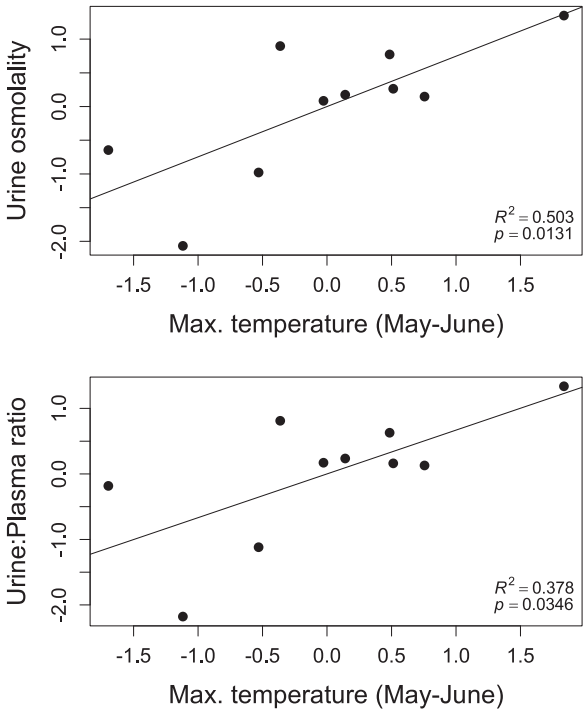

Figure 6. Linear regression results showing the relationship between the maximum average temperature (°C) for the months of May–June and urine osmolality and urine:plasma osmolality ratio. All values are *z*-transformed.

Variation in the nature or magnitude of relevant selection pressures across qualitatively similar environments has been shown to be the most important factor influencing patterns of nonparallelism in some systems (e.g., Berner et al. 2009; Langerhans 2018). In our trait-specific analyses, ecological factors (i.e., maximum temperature) only explained variation in traits associated with salt excretion (i.e., urine osmolality and urine:plasma osmolality ratio), and along with variation in migration rate, contributed significantly to variation in plasma osmolality among sites (Table 2). Environmental differences among sites did not explain variation in the direction of multivariate divergence among sites when accounting for variation in genetic structure, yet differences in the magnitude of environmental differences between interior and tidal marsh populations did explain variation in the magnitude of multivariate, osmoregulatory trait divergence. These multivariate results contrast with findings in stickleback fish, where the direction of phenotypic divergence was better explained by direction of ecological differences between habitats, but the magnitude of multivariate trait divergence was best explained by variation in genetic distance between populations (Stuart et al. 2017). These opposite results are not necessarily surprising given the many differences in the species, traits, and ecological variables measured between studies, but it does highlight the many ways in which patterns of adaptive divergence can be influenced by ecological and demographic processes.

Previous studies have also documented extensive variation in the degree of parallelism across traits (e.g., Kaeuffer et al. 2012; Stuart et al. 2017; Thompson et al. 2017; Langerhans 2018), but in many cases the analyzed traits contribute to different aspects of organismal performance making it difficult to understand how different evolutionary mechanisms contribute to variation in the degree of parallelism. In contrast, we focused on a suite of traits that contribute to the same metric of performance (i.e., osmoregulatory performance). This perspective can have important implications because we might expect that selection on differential fitness among individuals will shape variation in functionally integrated traits in a uniform way (e.g., Langerhans 2018). However, our results indicate that functionally integrated traits do not always respond to variation in the selective landscape or demographic variation in uniform ways. This suggests that differences in additional factors, such as the degree of trait plasticity (Wund et al. 2008; Dalziel et al. 2015; Oke et al. 2016) and/or the underlying genetic architecture (Yeaman and Whitlock 2011; Savolainen et al. 2013; Pfeifer et al. 2018) may further contribute to the different responses to environmental and demographic variation observed across traits.

A number of factors may influence interpretation of our results. First, the high levels of uncertainty around point estimates for migration rate and other demographic parameters may impact results. However, we also find a strong correlation between the migration rate estimated in ∂a∂i and estimates of Fst, suggesting point estimates of migration rate based on the SFS do reflect relative differences in the rate of gene flow experienced among tidal marsh populations. Moreover, SEM models performed with Fst instead of migration rate showed largely similar results (Table S5) further supporting the inference that gene flow likely constrains adaptive divergence in some traits. Second, gene flow will only be able to constrain phenotypic divergence if trait values are genetically determined (Lenormand 2002), and the traits we measured vary in the degree to which they are plastic in response to different temperature or salinity regimes (summarized in Table S1). For example, although plasma osmolality does not seem to vary across salinity treatments in acclimation studies of songbirds (including Savannah sparrows), other traits, such as medulla volume, exhibit substantial plasticity as well as genetic variation for the plastic response itself (e.g., Sabat et al. 2004; Peña-Villalobos et al. 2013; Benham 2018). Maximum urine concentrating ability is particularly affected by environmental factors and recent acclimatization history, and field measures of this trait are associated with high levels of variance (Table S4). Correlations between urine osmolality measures and maximum temperature across the 10 tidal marsh populations could reflect these direct environmental influences, but controlled experiments are needed for confirmation. Thus, although genetic variation likely explains a portion of the observed spatial variation in the osmoregulatory traits we examined,

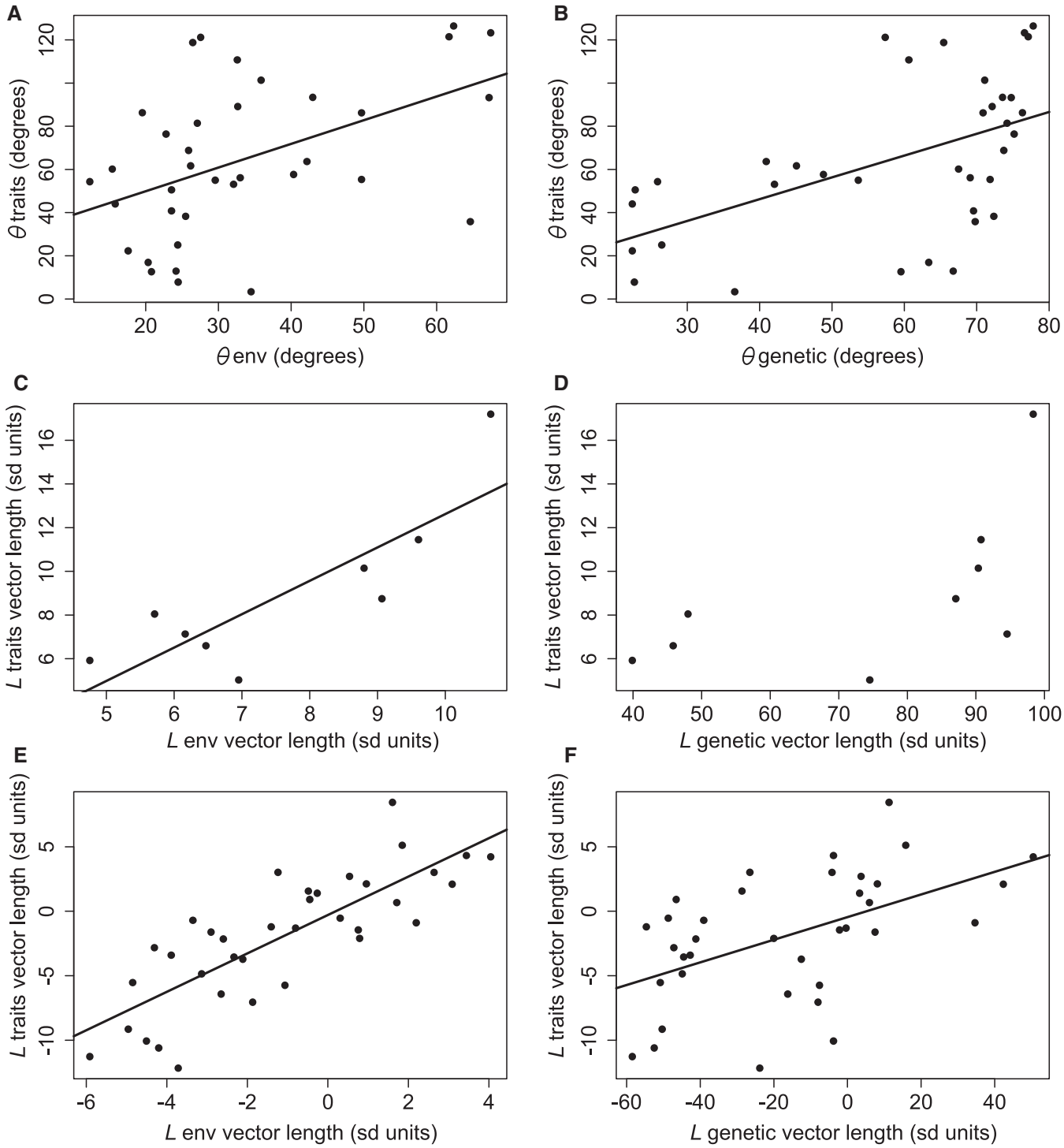

Figure 7. Comparisons of pairwise differences in the angle (θ), magnitude (*L*), and differences in magnitude (Δ*L*) of divergence vectors from interior populations for each of the 10 tidal marsh populations. (a) Pairwise differences in the angle between phenotypic vectors as explained by variation in the angle of environmental vectors and (b) in the angle of genetic distance vectors. (c) Variation in the magnitude of divergence for each population vector as explained by magnitude of environmental differences and (d) magnitude of genetic divergence. (e) Pairwise differences in the magnitude of divergence among phenotypic vectors of divergence as explained by pairwise differences in the magnitude of divergence of environment and (f) pairwise differences in the magnitude of genetic divergence. Significance of relationships (solid line = significant) between θ and Δ*L* evaluated using partial Mantel tests and *L* evaluated using linear regression.

phenotypic plasticity likely contributes as well. Nonetheless, the results of this study still shed light on the complex interactions among evolutionary forces that shape patterns of phenotypic divergence.

Conclusions

Our analyses show that both ecological variation among sites and variation in gene flow patterns contribute to variation in the magnitude and direction of divergence in traits contributing to osmoregulatory performance. These results highlight the empirical value of explicitly considering functionally integrated traits in studies assessing the degree of parallel adaptation to develop a more nuanced perspective on how different evolutionary processes might interact to shape adaptive outcomes. Additionally, this study contributes to the growing recognition that demography must be accounted for in studies of geographic variation (e.g., Stone et al. 2011; Roseman and Auerbach 2015). Although spatial correlations of phenotypic and environmental variation have long been interpreted as evidence for the importance of selection in shaping geographic variation (e.g., Mayr 1963; James 1970; Graves 1991), much of this work has traditionally ignored the potential influence of demography on patterns of intraspecific ecogeographic variation. Our approach for dissecting the relative contributions of environmental variation and demography in shaping spatial patterns of phenotypic variation should be broadly applicable, and contribute to an improved understanding of the diverse processes that drive patterns of phenotypic variation.

AUTHOR CONTRIBUTIONS

PMB and ZAC designed the study. PMB collected and analyzed all the data. PMB and ZAC wrote the paper.

ACKNOWLEDGMENTS

We thank the following museums and individuals for providing tissue samples for this study: J. Cracraft, P. Sweet, and T. Trombone (AMNH); J. Rising, R. Zink, and M. Westberg (ROM and BELL); P. Unitt and K. Burns (SDNHM & SDSU Museum of Biodiversity); S. Birks (UWBM). Adolfo Navarro-Siqüenza was instrumental in providing necessary permits and assistance with field logistics for work in Mexico. We also thank J. Bates, S. Hackett, B. Marks, J. Maley, J. McCormack, and A. Gordillo Martínez for their assistance with permits and field logistics. S. M. Robles Bello, A. Hernández Cardona, D. Levey, and D. Senner provided excellent field assistance in collecting samples. J. Jones and A. Hernandez helped with sequencing and lab work. L. Herritt, G. Carlson, and K. Booi for assistance with all hisotological procedures. C. Cheng for providing access to the osmometer in her laboratory. Personnel at CDFW and USFWS assisted with access to federal and state lands. Finally, we thank N. Sly, M. Stager, C. Wolf, R. Schweizer, J. Velotta, N. Senner, E. Beckman, Andrew Crawford, and three anonymous reviewers for valuable comments on the manuscript. Funding for field work and sequencing was provided by AMNH Frank M. Chapman Memorial Fund, SSE Rosemary Grant Award, SICB GIAR, Sigma-XI GIAR, UIUC Animal Biology departmental grants, Illinois Ornithological Society, Systematics Research Fund, AOU research award, Center for Latin America & Caribbean Studies Tinker Fellowship, and startup funds to ZAC from UM and UIUC.

DATA ARCHIVING

Short-read Illumina data have been submitted to the NCBI sequence read archive (SRA accession: PRJNA521441). All code and data used in analyses for this paper can be found on github at: https://github.com/phbenham/BenhamCheviron_evolution2019_DataCode

LITERATURE CITED

Adams, D. C., and M. L. Collyer. 2009. A general framework for the analysis of phenotypic trajectories in evolutionary studies. Evolution 63:1143–1154.

Agashe, D., J. J. Falk, and D. I. Bolnick. 2011. Effects of founding genetic variation on adaptation to a novel resource. Evolution 65:2481–2491.

Alfaro, M. E., D. I. Bolnick, and P. C. Wainwright. 2005. Evolutionary consequences of many-to-one mapping of jaw morphology to mechanics in labrid fishes. Am. Nat 165:E140–E154.

Allen, J. A. 1877. The influence of physical conditions in the genesis of species. Radical Rev. 1:108–140.

Arnold, S. J. 1983. Morphology, performance and fitness. Am. Zool. 23:347–361.

Bartholomew, G. A., and T. J. Cade. 1963. The water economy of land birds. Auk 80:504–539.

Beall, C. M. 2006. Andean, Tibetan, and Ethiopian patterns of adaptation to high-altitude hypoxia. Int. Comp. Biol. 46:18–24.

———. 2007. Two routes to functional adaptation: Tibetan and Andean high-altitude natives. Proc. Nat. Acad. Sci. USA 104:8655–8660.

Benham, P. M. 2018. Colonization of and adaptation to tidal marshes in the Savannah sparrow (*Passerculus sandwichensis*). Ph.D. Dissertation, University of Montana, Missoula, MT.

Benham, P. M., and C. C. Witt. 2016. The dual role of Andean topography in primary divergence: functional and neutral variation among populations of the hummingbird, *Metallura tyrianthina*. BMC Evol. Biol. 16:22.

Benham, P. M., and Z. A. Cheviron. 2019. Divergent mitochondrial lineages arose within a large, panmictic population of the Savannah sparrow (Passerculus sandwichensis). Mol. Ecol. https://doi.org/10.1111/mec.15049

Bergmann, C. 1847. Über die Verhältnisse der Wärmeökonomie der Thiere zu ihrer Grösse. Göttinger Studien 3:595–708.

Berner, D., A. C. Grandchamp, and A. P. Hendry. 2009. Variable progress toward ecological speciation in parapatry: stickleback across eight lake-stream transitions. Evolution 63:1740–1753.

Bolnick, D. I., R. D. H. Barrett, K. B. Oke, D. J. Rennison, and Y. E. Stuart. 2018. (Non) parallel evolution. Annu. Rev. Ecol. Syst. 49:303–330.

Cade, T., and G. A. Bartholomew. 1959. Sea-water and salt utilization by Savannah sparrows. Physiol. Zool. 32:230–238.

Casotti, G., and E. J. Braun. 2000. Renal anatomy in sparrows from different environments. J. Morphol. 243:283–291.

Casotti, G. 2001. Effects of season on kidney morphology in house sparrows. J. Exp. Biol. 204:1201–1206.

Catchen, J. M., A. Amores, P. Hohenlohe, W. Cresko, J. H. Postlethwait, and D. J. De Koning. 2011. Stacks: building and genotyping loci de novo from short-read sequences. G3: Genes|Genomes|Genetics 1:171–182.

Catchen, J., P. A. Hohenlohe, S. Bassham, A. Amores, and W. A. Cresko. 2013. Stacks: an analysis tool set for population genomics. Mol. Ecol. 22:3124–3140.

Coffman, A. J., P. H. Hsieh, S. Gravel, and R. N. Gutenkunst. 2016. Computationally efficient composite likelihood statistics for demographic inference. Mol. Biol. Evol. 33:591–593.

Dalziel, A. C., N. Martin, M. Laporte, H. Guderley, and L. Bernatchez. 2015. Adaptation and acclimation of aerobic exercise physiology in Lake Whitefish ecotypes (*Coregonus clupeaformis*). Evolution 69:2167–2186.

Dawson, W. R. 1982. Evaporative losses of water by birds. Comp. Biochem. Phys. A Physiol. 71:495–509.

deRivera, C. E. 2000. Belding's savannah sparrows eat eggs from live fiddler crabs. Wilson J. Ornithol. 112:427–428.

Fitzpatrick, S. W., J. C. Gerberich, L. M. Angeloni, L. L. Bailey, E. D. Broder, J. Torres-Dowdall, C. A. Handelsman, A. López-Sepulcre, D. N. Reznick, C. K. Ghalambor, et al. 2016. Gene flow from an adaptively divergent source causes rescue through genetic and demographic factors in two wild populations of *Trinidadian guppies*. Evol. Appl. 9:879–891.

Garant, D., S. E. Forde, and A. P. Hendry. 2007. The multifarious effects of dispersal and gene flow on contemporary adaptation. Func. Ecol. 21:434–443.

Goldstein, D. L. 2006. Osmoregulatory biology of saltmarsh passerines *in* terrestrial vertebrates of tidal marshes: evolution, ecology, and conservation. Stud. Avian Biol. 32:110–118.

Goldstein, D. L., and E. J. Braun. 1989. Structure and concentrating ability in the avian kidney. Am. J. Phys. 256:501–509.

Goldstein, D. L., J. B. Williams, and E. J. Braun. 1990. Osmoregulation in the field by salt-marsh savannah sparrows *Passerculus sandwichensis beldingi*. Phys. Zool. 63:669–682.

Gosselin, T., and L. Bernatchez. 2016. stackr: GBS/RAD data exploration, manipulation and visualization using R. R package version 0.4.6. https://github.com/thierrygosselin/stackr; https://doi.org/10.5281/zenodo.154432

Graves, G. R. 1991. Bergmann's rule near the equator: latitudinal clines in body size of an Andean passerine bird. Proc. Natl. Acad. Sci. USA 88:2322–2325.

Grinnell, J., and A. H. Miller. 1944. The distribution of the birds of California. Pacific Coast Avifauna 27:1–608.

Gundersen, H. J. G., T. F. Bendtsen, L. Korbo, N. Marcussen, A. Møller, K. Nielsen, J. R. Nyengaard, B. Pakkenberg, F. B. Sørensen, A. Vesterby, et al. 1988. Some new, simple and efficient stereological methods and their use in pathological research and diagnosis. Apmis 96:379–394.

Gutenkunst, R. N., R. D. Hernandez, S. H. Williamson, and C. D. Bustamante. 2009. Inferring the joint demographic history of multiple populations from multidimensional SNP frequency data. PLoS Genet. 5. https://doi.org/10.1371/journal.pgen.1000695

Hijmans, R. J., S. E. Cameron, J. L. Parra, P. G. Jones, and A. Jarvis. 2005. Very high resolution interpolated climate surfaces for global land areas. Int. J. Clim. 25:1965–1978.

Hohenlohe, P. A., S. Bassham, P. D. Etter, N. Stiffler, E. A. Johnson, and W. A. Cresko. 2010. Population genomics of parallel adaptation in threespine stickleback using sequenced RAD tags. PLoS Genet. 6. https://doi.org/10.1371/journal.pgen.1000862

James, F. C. 1970. Geographic size variation in birds and its relationship to climate. Ecology 51:365–390.

Johnson, O. W., and J. N. Mugaas. 1970. Quantitative and organizational features of the avian renal medulla. Condor 72:288–292.

Johnson, O. W., and R. D. Ohmart. 1973. Some features of water economy and kidney microstructure in the large-billed savannah sparrow (*Passerculus sandwichensis rostratus*). Phys. Zool. 46:276–284.

Kaeuffer, R., C. L. Peichel, D. I. Bolnick, and A. P. Hendry. 2012. Parallel and nonparallel aspects of ecological, phenotypic, and genetic divergence across replicate population pairs of lake and stream stickleback. Evolution 66:402–418.

Kawecki, T. J., and D. Ebert. 2004. Conceptual issues in local adaptation. Ecol. Lett. 7:1225–1241.

Langerhans, R. B. 2018. Predictability and parallelism of multitrait adaptation. J. Heredity 109:59–70.

Leimu, R., and M. Fischer. 2008. A metaanalysis of local adaptation in plants. PLoS ONE 3:1–8.

Leinonen, T., R. J. S. McCairns, G. Herczeg, and J. Merilä. 2012. Multiple evolutionary pathways to decreased lateral plate coverage in freshwater threespine sticklebacks. Evolution 66:3866–3875.

Lenormand, T. 2002. Gene flow and the limits to natural selection. Trends Ecol. Evol. 17:183–189.

Mayr, E. 1963. Animal species and evolution. Harvard Univ. Belknap Press, Cambridge, MA.

McKechnie, A. E., and B. O. Wolf. 2004. Partitioning of evaporative water loss in white-winged doves: plasticity in response to short-term thermal acclimation. J. Exp. Biol. 207:203–210.

Mopper, S., P. Stiling, K. Landau, D. Simberloff, and P. Van Zandt. 2000. Spatiotemporal variation in leafminer population structure and adaptation to individual oak trees. Ecology 81:1577–1587.

Nosil, P., and B. J. Crespi. 2004. Does gene flow constrain adaptive divergence or vice versa? A test using ecomorphology and sexual isolation in *Timena cristinae* walking-sticks. Evolution 58:102–112.

Oke, K. B., M. Bukhari, R. Kaeuffer, G. Rolshausen, K. Räsänen, D. I. Bolnick, C. L. Peichel, and A. P. Hendry. 2016. Does plasticity enhance or dampen phenotypic parallelism? A test with three lake-stream stickleback pairs. J. Evol. Biol. 29:126–143.

Oke, K. B., G. Rolshausen, C. LeBlond, and A. P. Hendry. 2017. How parallel is parallel evolution? A comparative analysis in fishes. Am. Nat. 190: 1–16.

Parchman, T. L., Z. Gompert, J. Mudge, F. D. Schilkey, C. W. Benkman, and C. A. Buerkle. 2012. Genome-wide association genetics of an adaptive trait in lodgepole pine. Mol. Ecol. 21:2991–3005.

Peña-Villalobos, I., F. Valdés-Ferranty, and P. Sabat. 2013. Osmoregulatory and metabolic costs of salt excretion in the Rufous-collared sparrow *Zonotrichia capensis*. Comp. Biochem. Physiol. 164:314–318.

Pfeifer, S. P., S. Laurent, V. C. Sousa, C. R. Linnen, M. Foll, L. Excoffier, H. Hoekstra, and J. D. Jensen. 2018. The evolutionary history of Nebraska Deer mice: local adaptation in the face of strong gene flow. Mol. Biol. Evol. 35:792–806.

Postma, E., and A. J. van Noordwijk. 2005. Gene flow maintains a large genetic difference in clutch size at a small spatial scale. Nature 433:65–68.

Poulson, T. L. 1965. Countercurrent multipliers in avian kidneys. Science 14:389–391.

Poulson, T. L., and G. A. Bartholomew. 1962. Salt balance in the Savannah sparrow. Phys. Zool. 35:109–119.

Raeymaekers, J. A. M., N. Konijnendijk, M. H. D. Larmuseau, B. Hellemans, L. De Meester, and F. A. M. Volckaert. 2014. A gene with major phenotypic effects as a target for selection vs. homogenizing gene flow. Mol. Ecol. 23:162–181.

Räsänen, K., and A. P. Hendry. 2008. Disentangling interactions between adaptive divergence and gene flow when ecology drives diversification. Ecol. Lett. 11:624–636.

Rosseel, Y. 2012. Lavaan: an R package for structural equation modeling. J. Statist. Softw. 48:1–36.

Roseman, C. C., and B. M. Auerbach. 2015. Ecogeography, genetics, and the evolution of human body form. J. Human Evol. 78:80–90.

Sabat, P., K. Maldonado, A. Rivera-Hutinel, and G. Farfan. 2004. Coping with salt without salt glands: osmoregulatory plasticity in three species

of coastal songbirds (ovenbirds) of the genus Cinclodes (Passeriformes: Furnariidae). J. Comp. Phys. B Biochem. Syst. Env. Phys. 174:415–420.

Savolainen, O., M. Lascoux, and J. Merilä. 2013. Ecological genomics of local adaptation. Nat. Rev. Gen. 14:807–820.

Schneider, C. A., W. S. Rasband, and K. W. Eliceiri. 2012. NIH Image to ImageJ: 25 years of image analysis. Nat. Meth. 9:671–675.

Slatkin, M. 1987. Gene flow and the geographic structure of natural populations. Science 236:787–792.

Stone, G. N., S. Nee, and J. Felsenstein. 2011. Controlling for non-independence in comparative analysis of patterns across populations within species. Phil. Tran. Roy. Soc. B Biol. Sci. 366:1410–1424.

Storz, J. F., G. R. Scott, and Z. A. Cheviron. 2010. Phenotypic plasticity and genetic adaptation to high-altitude hypoxia in vertebrates. J. Exp. Biol. 213:4125–4136.

Stuart, Y. E., T. Veen, C. Thompson, T. Tasneem, N. Ahmed, R. Izen, N. Ahmed, R. D. H. Barrett, A. P. Hendry, C. L. Peichel, et al. 2017. Contrasting effects of environment and genetics generate a predictable continuum of parallel evolution. Nat. Ecol. Evol. 1:1–7.

Thompson, C. J., N. I. Ahmed, T. Veen, C. L. Peichel, A. P. Hendry, D. I. Bolnick, and Y. E. Stuart. 2017. Many-to-one form-to-function mapping weakens parallel morphological evolution. Evolution 71:2738–2749.

van Rossem, A. J. 1947. A synopsis of the Savannah sparrows of Northwestern Mexico. Condor 49:97–107.

Velotta, J. P., J. L. Wegrzyn, S. Ginzburg, L. Kang, S. Czesny, R. J. O'Neill, S. D. McCormick, P. Michalak, and E. T. Schultz. 2017. Transcriptomic imprints of adaptation to fresh water: parallel evolution of osmoregulatory gene expression in the Alewife. Mol. Ecol. 26:831–848.

Walsh, J., P. M. Benham, P. E. Deane-Coe, P. Arcese, B. G. Butcher, Y. L. Chan, Z. A. Cheviron, C. S. Elphick, A. I. Kovach, B. J. Olsen, et al. 2019. Genomics of rapid ecological divergence and parallel adaptation in four tidal marsh sparrows. Evol. Lett. 3:324–338. https://doi.org/10.1002/evl3.126

Weber, K. E., and L. T. Diggins. 1990. Increased selection response in larger populations. II. Selection for ethanol vapor resistance in *Drosophila melanogaster* at two population sizes. Genetics 125:585–597.

Weir, B. S., and C. C. Cockerham. 1984. Estimating F-statistics for the analysis of population structure. Evolution 38:1358–1370.

Wheelwright, N. T., and J. D. Rising. 2008. Savannah sparrow (*Passerculus sandwichensis*). *in* A. Poole, ed. Birds of North American online. Cornell Lab of Ornithology, Ithaca, NY. https://doi.org/10.2173/bna.45

Whiteley, A. R., S. W. Fitzpatrick, W. C. Funk, and D. A. Tallmon. 2015. Genetic rescue to the rescue. Trends Ecol. Evol. 30:42–49.

Williams, J. B., and B. I. Tieleman. 2005. Physiological adaptation in desert birds. BioScience 55:416–425.

Williams, J. B., A. Munoz-Garcia, and A. Champagne. 2012. Climate change and cutaneous water loss of birds. J. Exp. Biol. 215:1053–1060.

Wright, S. 1982. Character change, speciation, and the higher taxa. Evolution 36:427–443.

Wund, M. A., J. A. Baker, B. Clancy, J. L. Golub, and S. A. Foster. 2008. A test of the "Flexible Stem" model of evolution: ancestral plasticity, genetic accommodation, and morphological divergence in the threespine stickleback radiation. Am. Nat. 172:449–462.

Yarbrough, C. G. 1971. The influence of distribution and ecology on the thermoregulation of small birds. Comp. Biochem. Phys. A Phys. 39:235–266.

Yeaman, S., and M. C. Whitlock. 2011. The genetic architecture of adaptation under migration-selection balance. Evolution 65:1897–1911.

Zhang, G., C. Li, Q. Li, B. Li, D. M. Larkin, C. Lee, J. F. Storz, A. Antunes, M. J. Greenwold, R. W. Meredith, et al. 2014. Comparative genomics reveals insights into avian genome evolution and adaptation. Science 346:1311–1320.

Zink, R. M., J. D. Rising, S. Mockford, A. G. Horn, J. M. Wright, M. Leonard, and M. C. Westberg. 2005. Mitochondrial DNA variation, species limits, and rapid evolution of plumage coloration and size in the Savannah sparrow. Condor 107:21–28.

Associate Editor: A. J. Crawford
Handling Editor: M. R. Servedio

Supporting Information

Additional supporting information may be found online in the Supporting Information section at the end of the article.

Table S1. Evidence for plasticity in osmoregulatory traits in response to salinity, humidity, or temperature variation across different passerine species.
Table S2. Specimen vouchers, tissue samples, and locality information for individuals sampled for physiological and/or sequence data.
Table S3. Environmental data from each sampling locality.
Table S4. Mean trait values for each sampled population with standard deviation in parentheses.
Table S5. Structural equation modeling results examining relative influence of ecology and genetic divergence on trait divergence across the 10 tidal marsh populations (see Fig. 2).
Figure S1. Linear regression results showing the relationship between effective population size and each of the measured osmoregulatory traits.
Figure S2. Correlation matrix among each of the six physiological traits.
Figure S3. Regression analyses showing influence of migration rate and divergence times on Fst variation in tidal marsh Savannah sparrows.